◆ Human Brain Mapping 7:49–66(1999) ◆

Lateralized Auditory Spatial Perception and the Contralaterality of Cortical Processing as Studied With Functional Magnetic Resonance Imaging and Magnetoencephalography

Marty G. Woldorff,[1,3]* Claus Tempelmann,[1,2] Juergen Fell,[2] Carola Tegeler,[1] Birgit Gaschler-Markefski,[1] Hermann Hinrichs,[2] Hans-Jochen Heinze,[2] and Henning Scheich[1]

[1]*Federal Institute for Neurobiology, Magdeburg, Germany*
[2]*Clinical Neurophysiology, Otto-von-Guericke University, Magdeburg, Germany*
[3]*Research Imaging Center, University of Texas Health Science Center, San Antonio, TX, USA*

Abstract: Functional magnetic resonance imaging (fMRI) and magnetoencephalography (MEG) were used to study the relationships between lateralized auditory perception in humans and the contralaterality of processing in auditory cortex. Subjects listened to rapidly presented streams of short FM-sweep tone bursts to detect infrequent, slightly deviant tone bursts. The stimulus streams consisted of either monaural stimuli to one ear or the other or binaural stimuli with brief interaural onset delays. The onset delay gives the binaural sounds a lateralized auditory perception and is thought to be a key component of how our brains localize sounds in space. For the monaural stimuli, fMRI revealed a clear contralaterality in auditory cortex, with a contralaterality index (contralateral activity divided by the sum of contralateral and ipsilateral activity) of 67%. In contrast, the fMRI activations from the laterally perceived binaural stimuli indicated little or no contralaterality (index of 51%). The MEG recordings from the same subjects performing the same task converged qualitatively with the fMRI data, confirming a clear monaural contralaterality, with no contralaterality for the laterally perceived binaurals. However, the MEG monaural contralaterality (55%) was less than the fMRI and decreased across the several hundred millisecond poststimulus time period, going from 57% in the M50 latency range (20–70 ms) to 53% in the M200 range (170–250 ms). These data sets provide both quantification of the degree of contralaterality in the auditory pathways and insight into the locus and mechanism of the lateralized perception of spatially lateralized sounds. *Hum. Brain Mapping 7:49–66, 1999.*

Key words: auditory cortex; contralateral; perception; fMRI; MEG; auditory space; interaural time delay

INTRODUCTION

The mammalian auditory cortex in one hemisphere receives input from both ears and is activated by sounds in both hemispaces [Brodal, 1981]. The auditory system is thus not as contralateral as the somato-

Contract grant sponsor: the German BMBF.

*Correspondence to: Marty G. Woldorff, Ph.D., University of Texas Health Science Center, Research Imaging Center, 7703 Floyd Curl Dr., San Antonio, TX 78282–6240. E-mail: mwoldorff@uthscsa.edu or marty.woldorff@ifn-magdeberg.de

Received 6 February 1998; accepted 7 August 1998

sensory system in terms of the receptors, and not as contralateral as the visual system in terms of the hemispace. The ascending auditory pathways coming from the two ears do cross at various levels in the brainstem, including the outputs of the cochlear nuclei, the superior olivary nuclei, and the inferior colliculi. At each of these levels, however, this crossing is not complete and many fibers also project ipsilaterally. This leads to both ipsilateral and contralateral representations at the various processing stages, including auditory cortex, after which even more crossing can occur via the corpus callosum.

On the other hand, the animal neurophysiological and neuroanatomical literature has provided abundant data to show that, although there is auditory representation from both ears to both cortices, the contralateral pathways and excitatory representations are generally greater than the ipsilateral [reviewed in Pickles, 1981; Irvine, 1992; Winer, 1992; Clarey at al., 1992; King and Carlisle, 1995]. For example, neuroanatomical pathway tracing studies in cats and rodents have estimated that there are more fibers crossing at the various brainstem relay centers than projecting ipsilaterally. In addition, mammalian neurophysiological studies recording from cells in auditory cortex have indicated greater excitatory responses to contralateral than to ipsilateral stimuli. This dominance is related to the existence of EE cells, which are excited by stimuli to both ears but usually more strongly by the contralateral ear, and EI cells, which are excited by contralateral-ear stimuli and inhibited by ipsilateral-ear ones.

Lesion studies also seem to indicate a contralateral predominance in the mammalian auditory system, although this appears to be more related to processing in the contralateral hemispace, rather than the contralateral ear. More specifically, although the bilateral representation in auditory cortex appears to keep lesions in one auditory cortex from substantially reducing the hearing acuity for sounds in the contralateral ear, such unilateral lesions do markedly reduce the ability to localize and attend to sounds within contralateral space [Jenkins and Masterton, 1982; reviewed in Pickles, 1981; Clarey et al., 1992; King and Carlisle, 1995].

Relatively few human studies have focused on assessing auditory contralaterality. A few direct intracranial recordings have investigated contralaterality and have reported evoked potentials to be ~30% larger contralaterally [Celesia, 1976]. Scalp electrical recordings have reported that the large event-related potential (ERP) N100 component (at ~100 msec), along with the earlier P30 wave, tends to be only slightly larger contralaterally (~10%) [reviewed in Naatanen and Picton, 1987]. However, electrical volume conduction is likely to dilute the contralateral/ipsilateral differences of these components, especially at the scalp. Accordingly, studies using magnetoencephalography (MEG), which can more selectively assess the electrophysiological responses within a sulcus (such as the Sylvian fissure) undistorted by volume conduction from the other side of the head [Hamalainen et al., 1993], have reported that the M100 component to monaural sounds is ~15–30% larger over contralateral auditory cortex [Pantev et al., 1986; Makela et al., 1993]. Few studies using positron emission tomography (PET) or functional magnetic resonance imaging (fMRI) have assessed the contralaterality of auditory cortex processing, although a number have reported auditory cortex activations in response to sounds [e.g., Lauter et al., 1985; Binder et al., 1994; Zatorre et al., 1994].

Although brain recordings during monaural auditory stimulation enable assessment of the contralaterality of the auditory pathways, in the real world few sounds are totally monaural. Rather, sounds come from different locations in space, and the brain uses interaural onset, phase, and intensity differences to help localize the sounds [reviewed in Moore, 1994; Blauert, 1997]. Key initial parts of this analysis are known to occur in the superior olivary nuclei in the brainstem, but neuronal units in other areas, including the auditory cortex, reflect binaural interactions related to these interaural auditory features (e.g., EE and EI units). However, the locus of the auditory spatial perception itself is not known, nor is it generally clear how the single-unit activity recorded in animal studies would be reflected in the various macroscopic population brain recordings now possible in humans.

In the present study, fMRI based on the blood-oxygen-level-dependent (BOLD) signal and MEG were used to study the relationships between lateralized auditory perception in humans and the contralaterality of processing in auditory cortex. There were three main questions: 1) How contralateral is the processing in human auditory cortex of monaural stimuli, which are clearly perceived as highly lateralized? 2) How contralateral is the processing of binaural stimuli that are laterally perceived due to having short interaural onset delays (~2 msec)? 3) How well do fMRI (a hemodynamic measure) and MEG (an electrical/magnetic measure) correspond in their assessment of this processing and its contralaterality?

METHODS

Stimuli and task

Functional MRI and MEG recordings of brain activity were recorded (in separate sessions) while subjects (n = 9, ages 18–41 years) either rested with eyes closed or listened to brief, rapidly presented, 73-dBSPL, FM-sweep tone bursts to detect infrequent deviant bursts (also with eyes closed). Each of the (nontarget) monaural tone bursts was 20 msec in duration and was composed of a sequence of seven partially overlapping subcomponent tone pips that were 500 Hz, 700 Hz, 1000 Hz, 1400 Hz, 2000 Hz, 2800 Hz, and 4000 Hz, with a 2 msec delay between the onsets of successive subcomponents. Each of these subcomponents was 8 msec in duration, and was shaped in a ''3–2-3'' pattern (3-msec onset, 2-msec plateau, and 3-msec decay). Thus, these tone bursts sounded like brief upward-going FM-sweeps. These particular stimuli were used as a compromise for the two methodologies to be used: preliminary observations from our laboratory indicated that longer sounds that cover a broader frequency range (such as FM-sweeps) appeared to give greater activations in fMRI than brief simple tone pips, but brief transient sounds are still needed to evoke reliable MEG transient responses, as they are mainly responsive to stimulus onsets [Naatanen and Picton, 1987]. Thus, we found that these stimuli could elicit robust responses in both recording modalities. In addition, FM-sweeps are important real-world auditory stimulus features for animal communication and human speech.

The binaural tone bursts were identical in structure to the monaural ones except that the input to one ear lagged the other ear by 2 msec, giving a striking lateralization of the auditory perception to the side of the leading ear. Although this onset delay is larger than would occur in the real world for a lateralized sound (which would be under 1 ms), this delay was chosen for several reasons: 1) perceptual lateralization tend to be slightly larger for onset delays that are somewhat larger than is physiologically plausible [Pickles, 1981; Blauert, 1997]; 2) based on preliminary testing in our laboratory, the degree of perceived lateralization of our stimuli due to onset delay alone was clearly somewhat larger for 2 ms than for 1 ms; and 3) we were trying to maximize perceptual lateralization in order to maximize our chances of detecting whether there was a corresponding lateralization in auditory cortex activity during such a percept.

The streams of FM-sweep sounds were presented at fairly rapid rates, with interstimulus intervals (ISIs) varying randomly (''jittered'') from 150–450 msec. Again, this stimulus rate structure was a compromise between the two modalities. Faster rates of stimulus presentation (shorter ISIs) evoke larger responses in the fMRI because it integrates activity across time, but faster rates generally yield smaller event-related fields (ERFs) (although having more stimulus trials to average partially makes up for the smaller signals). Shorter ISIs also result in overlap of the ERF responses from adjacent stimuli in the sequence, which can distort the final ERF time-locked averages. By jittering the ISIs across a wide range, however, this distortion can be greatly reduced, allowing extraction of relatively undistorted transient evoked MEG responses [Woldorff, 1993]. The infrequent (9%) deviant tones to be detected had a pitch difference (a decrease) in the final component of the seven-component FM sweeps. The size of this pitch deviance was adjusted for each subject to achieve a detection rate of about 80%; the typical deviance used was a reduction of the last subcomponent from 4000 Hz to ~3200 Hz.

fMRI recording

Five forward-tilting coronal slices were acquired with a FLASH conventional gradient-echo pulse sequence using a 3-Tesla Bruker headscanner. The slice thickness was 8 mm, matrix size 64 × 40, and field-of-view 16 cm. The TR / TE / flip angle values were 275 ms / 40 ms / 10 deg, and the time for acquiring a sample from all five slices was 11 sec. The five slices were chosen such that they were perpendicular to the Sylvian fissure (and thus auditory cortex) and such that the second most posterior slice went through the inferior colliculus (Fig. 1). Data were acquired in two subsessions, a monaural one and a binaural one. In the monaural subsession, each condition-cycle consisted of four phases in one of two orders: 1) left monaural, rest, right monaural, rest; or 2) right monaural, rest, left monaural, rest. Five samples were acquired in each of the left and right monaural phases, and three samples in each of the rest phases, so that one full cycle took ~3 min ((5+3+5+3)samples × 11 sec / sample). The binaural subsessions were identical in structure to the monaural ones, but with left monaural tones replaced by ''left binaural tones'' (i.e., left leading ear, thereby leading to left lateralized perception) and right

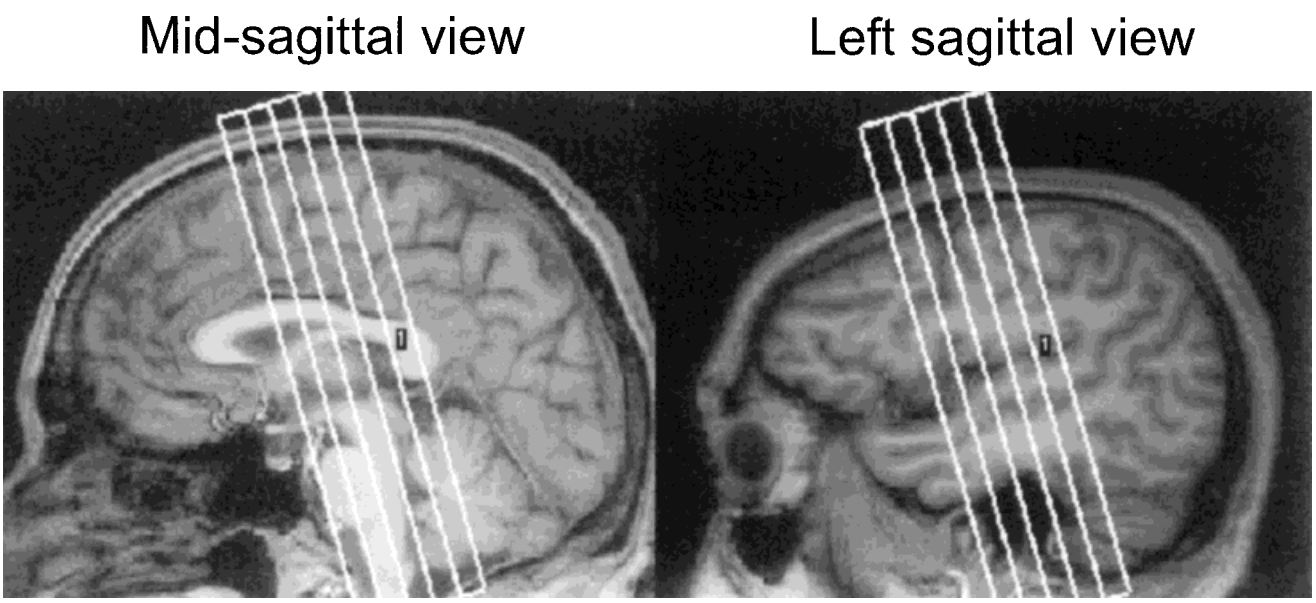

Figure 1.
Two sagittal MR views, one midsagittal and the other through the auditory cortex, showing the location and angle of the five forward-tilting slices for the fMRI recordings. These slices were selected so that they were as perpendicular as possible to the Sylvian fissure (and, thus, auditory cortex) and so that the second most posterior slice went through the inferior colliculus.

monaural tones by ''right binaural tones'' (right leading ear, right-side perception). Ten cycles were run in each subsession, with the left and right stimulus phases of the cycles in counterbalanced order. The sound level of the background acoustic noise due to the MRI scanner was measured and determined to be ~58 dB SPL.

MEG recording

Two sensor arrays, each with 37 first-order MEG gradiometers (Biomagnetic Technologies, Inc., San Diego, CA) were used to record evoked field responses, one array over each auditory cortex. One of the array dewars sat on the floor angled upward, and the subject laid on his or her side with the side of the head placed on that dewar such that it was centered over auditory cortex. The second dewar was then brought down from above so that the sensor array lay over the other auditory cortex. The side on which the subjects laid was always the same for both the monaural and binaural runs for each subject, but was counterbalanced across subjects. Each 37-channel dewar spanned a circular area of 144 mm diameter. A transceiver-based system was used to localize three skull landmarks (nasion and preauricular points) with respect to the magnetic sensor arrays. In addition, the head shape of each subject was digitized, which was used to derive best-fit local spheres for the dipole fit procedures. The MEG signals were continuously recorded (bandpass 1–50 Hz, digitization rate 208 Hz) and stored on disk along with the event codes for off-line time-locked selective averaging and analysis. The structure of the runs and the conditions was identical to that used in the fMRI.

fMRI analysis

Correlations of the fMRI data vs. the condition-cycle function were performed, separately for the left tones vs. rest and for right tones vs. rest. In each case, the first set of slice acquisitions (i.e., 11 sec) in each cycle phase were omitted from the analysis to allow for the hemodynamic delay of the BOLD effect after a condition change, leaving a total of 40 samples for each slice in each condition.

To assess the contralaterality of processing, intensity-weighted volumes of significantly activated pixels (i.e., number of significantly activated pixels times the average percent signal increase of those pixels) were

calculated (separately for pixel significances of $P < .01$ and $P < .05$) in rectangular regions of interest (ROIs) covering auditory cortex in each auditory stimulus condition vs. rest. The rectangular ROIs were defined as follows: upper border = Sylvian fissure, height = 2.5 cm, lateral border = lateral surface of brain, medial border = just lateral to insula. The most anterior slice of the five was not included in these ROIs because it had very few activated pixels under any of the stimulus conditions. Intensity-weighted volumes were calculated because they would take into account both intensity and extent effects, and contralaterality could presumably affect either or both of these. From these values a contralaterality index (activation from contralateral stimulation divided by the sum of the activations from contralateral and ipsilateral stimulation) was calculated for the monaural stimuli and for the lateralized binaural stimuli for each subject. These contralaterality index values were statistically compared to their ipsilateral counterparts across subjects using Wilcoxon matched-pairs signed-ranks tests. In addition, a two-factor repeated-measures analysis of variance (ANOVA) across subjects of the intensity-weighted-volume values themselves was performed, with Ear of Stimulation and Hemisphere as the factors. Lastly, for each subject the single-sample (i.e., single-acquisition) mean signal values of the significantly activated pixels in the ROI were entered into an ANOVA to assess the significance of contralaterality for each subject. The significantly activated pixels in the auditory cortex ROIs were overlaid on structural MRIs, enabling relationships to be drawn to high-resolution images of the anatomy.

The functional activations were also grand-averaged across subjects in the following way: The auditory cortex ROIs were all about the same size (10 pixels high, 4 pixels / slices anterior–posterior, 13 or 14 pixels deep); those that had an extra pixel in depth were trimmed on the medial side to match the rest. The series of MR signals in each of these pixels were then averaged across subjects, to give one sequence of signals in the various conditions to analyze with correlations. The same type of correlation of the fMRI signals vs. the conditions function was run on these data, thresholded at $P < .01$, and the significantly activated pixels from these grand-average activation patterns were then overlaid on a single subject's MRI anatomical scan for reference purposes. Based on the location of the ROI boundaries, the ROI could be located in Talairach atlas space [Talairach and Tournoux, 1988], allowing for a transformation to be created from the ROI pixel locations to Talairach space. This then allowed the center-of-mass locations of the grand-average functional activations to be expressed in approximate Talairach coordinates.

MEG analysis

The MEG signals were digitally low-pass filtered at 30 Hz, as well as passed through a noise reduction algorithm for subtraction of environmental noise using the information from eight reference channels [Robinson, 1989]. For each subject, averaged event-related field (ERF) waveforms were obtained to the standard and deviant tones under each stimulus condition. Trials with artifacts (field amplitude ranges larger than 2.5 pT) were rejected from the averages. Occasionally, one or two of the magnetic sensors in a dewar's array would fail or have unacceptably elevated noise levels and would be excluded from the analysis.

A grand average of the ERF responses at the extremum sites was also derived. For this, the ERF responses at the field maximum site and the field minimum site for each stimulus type, for each hemisphere, were extracted for each subject, and these were then averaged across subjects. Such an extraction and averaging approximately adjusts for variability in the sensor-array placement and in the anatomy of the individual subjects.

The contralaterality of the ERF responses was quantified in several different ways. Contralaterality indices were derived from the root-mean-square (RMS) of the field amplitudes of the standard-tone ERFs across all the channels over each hemisphere, integrated across specific latency windows centered on the major activity peaks believed to derive from auditory cortex (M50:20–70 ms, M100:80–160 ms, M200:170–250ms), as well as across the entire epoch encompassing these peaks (20–250 ms). As with the fMRI, the indices were computed as the contralateral activation measure divided by the sum of the contralateral and ipsilateral measures. Additional analyses were performed to determine whether there were any significant differences in the degree of contralaterality between the different latency windows.

Contralaterality indices were also derived from dipole-moment amplitudes of best-fitting equivalent current dipoles (ECDs), which were calculated in the

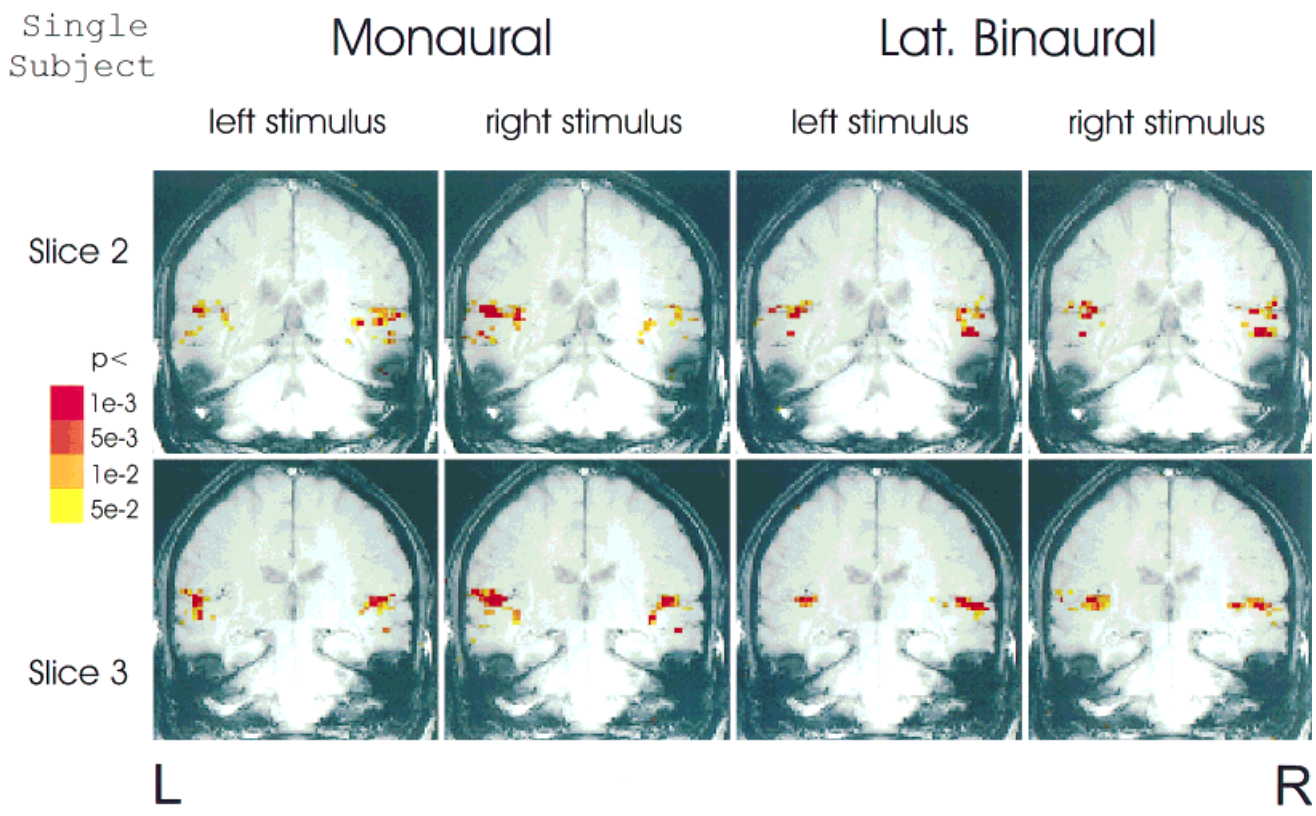

Figure 2.

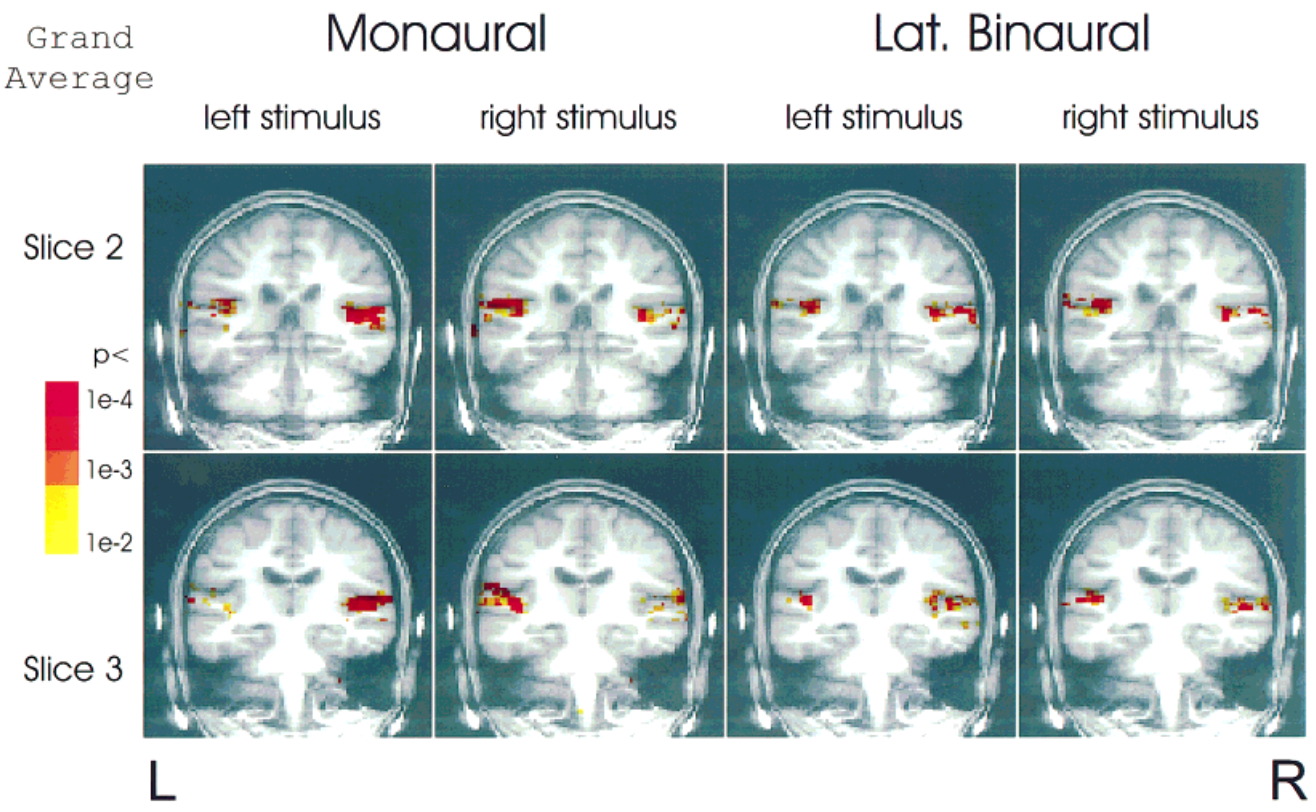

Figure 3.

following way. For each stimulus type, for each major component thought to arise from auditory cortex on the superior temporal plane, a best-fitting ECD for the surface field distribution over each hemisphere was calculated in the MEG reference frame (a frame based on three fiducial skull landmarks), using an algorithm based on least-squares approximation [Marquardt, 1963]. No location constraint was placed on this analysis, but the criteria for finding the ECD was as follows: Within the above-specified latency windows for the M50, M100, and M200, the ECD was calculated for each time point. The best-fitting ECD was then chosen as the one for the time point in that window that had the largest RMS value across the sites, for which the ECD had a confidence volume smaller than 8 cm^3 and a goodness of fit better than 85%.

Additional analyses were also performed to directly compare the degree of contralaterality as gauged by our fMRI measures to that gauged by our MEG measures.

RESULTS

fMRI data

The thresholded fMRI BOLD responses in auditory cortex to the monaural and binaural stimuli for slices 2 and 3 are shown for a single subject in Figure 2, overlaid on that subject's structural MRI scan. Figure 3 shows the analogous grand-average fMRI responses (see Methods). These figures illustrate the main pattern observed — namely, that the monaural stimuli gave a clear contralaterality effect, with the laterally perceived binaural stimuli showing little contralaterality. For this particular single subject, the monaural contralaterality index was .70; for the grand averaged data it was .69.

Figure 2.
fMRI activation in the auditory cortices for a single subject, overlaid on his/her structural MR scan, shown for slices 2 and 3. Activations shown consist of all pixels in the auditory cortex ROIs in these two slices that were significantly activated ($P < .01$) during the various auditory stimulus conditions. Activation in areas outside of the auditory cortex ROIs are not shown. Note that the monaural stimuli showed a contralaterality of processing, whereas the onset-delay binaural stimuli showed approximately equal activation for both the left-lateralized and right-lateralized sounds.

Figure 3.
fMRI activation in auditory cortex, grand-averaged across subjects, shown for slices 2 and 3. The series of MR signals in each of the pixels of the auditory cortex ROIs were averaged across subjects, to give one sequence of signals across the various stimulus conditions. Correlations were run on these data, thresholded at $P < .01$, and the significantly activated pixels from these grand-average activation patterns were then overlaid on a single subject's MRI anatomical scan for reference purposes. Activation in areas outside of the auditory cortex ROIs were not grand-averaged and are not shown. Note the strong contralaterality for the monaural stimuli, with approximately equal activation in the two auditory cortices for the onset-delay binaural stimuli.

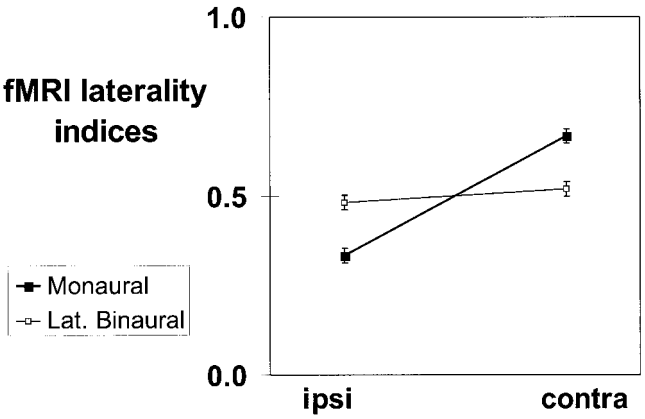

Figure 4.
Plots of the mean fMRI contralaterality indices (with SEM error bars) for the monaural stimuli and for the onset-delay, laterally perceived, binaural stimuli.

The statistical analysis of the individual subjects' contralaterality indices confirmed these observed patterns (Figure 4). The monaural contralaterality indices averaged across subjects was .67 ($\pm$SEM = .02) for $P <$ .01 and .61 ($\pm$SEM = .02) for pixels with $P < .05$. These results can also be viewed as indicating that the contralateral activation (e.g., .67) was about twice as large as the ipsilateral (.33 = 1–.67). Statistical analysis confirmed the contralaterality, in that a Wilcoxon matched-pairs signed-ranks test of the contralateral indices vs. ipsilateral indices was highly significant ($P < .005$). Lastly, a direct two-factor repeated-measures ANOVA of the intensity-weighted activation values themselves with factors of Ear and Hemisphere likewise gave a highly significant interaction ($F(1,8) = 37.4$, $P < .0003$).

In sharp contrast to the monaural stimuli, the perceptually lateralized onset-delay binaural tones did not give significantly greater fMRI activation in contralateral auditory cortex (Figs. 2, 3, 4). There was a very slight tendency for contralaterality (mean contralaterality index = .51 ($\pm$SEM = .02) for $P < .01$ and .52 ($\pm$SEM = .02) for $P < .05$, but this did not approach significance in analyses of either the

TABLE I. Talairach coordinates of the centers-of-mass of the fMRI activations: locations are in mm ±SEM

	Hemisphere	Stimulus	x (±SEM)	y (±SEM)	z (±SEM)
Mean of single subjects	Left	Mon. Left	−48 (±1.5)	−25 (±1.2)	9 (±1.2)
Grand-averaged activations	Left	Mon. Left	−47	−26	10
Mean of single subjects	Left	Mon. Right	−48 (±0.9)	−26 (±1.6)	9 (±1.3)
Grand averaged activations	Left	Mon. Right	−48	−25	10
Mean of single subjects	Right	Mon. Left	49 (±0.6)	−24 (±1.0)	10 (±0.8)
Grand averaged activations	Right	Mon. Left	48	−24	9
Mean of single subjects	Right	Mon. Right	49 (±1.3)	−24 (±1.5)	10 (±1.4)
Grand averaged activations	Right	Mon. Right	50	−25	9
Mean of single subjects	Left	Bin. Left	−48 (±1.0)	−27 (±1.4)	11 (±1.5)
Grand averaged activations	Left	Bin. Left	−46	−27	12
Mean of single subjects	Left	Bin. Right	−48 (±1.3)	−25 (±1.5)	10 (±1.5)
Grand averaged activations	Left	Bin. Right	−46	−26	12
Mean of single subjects	Right	Bin. Left	50 (±1.3)	−23 (±0.9)	11 (±0.9)
Grand averaged activations	Right	Bin. Left	50	−24	10
Mean of single subjects	Right	Bin. Right	50 (±.7)	−25 (±1.2)	8 (±1.4)
Grand averaged activations	Right	Bin. Right	51	−25	8

intensity-weighted activation volumes or of the indices.

In the single-subjects statistical analyses, the monaural stimuli produced activations that were significantly contralateral in seven of the nine subjects, with the results for the other two subjects approaching but not reaching significance. The activations produced by the onset-delay bilateral stimuli, on the other hand, did not reach significance in any of the single subjects.

The Talairach coordinates for the centers-of-mass of the fMRI activations calculated for each stimulus condition, for each subject, are given in Table 1, along with the corresponding centers-of-mass of the grand-averaged fMRI activations. These coordinates indicate that the centroid locations for the contralateral and ipsilateral stimulation did not differ, nor did the centroid locations for the monaural stimuli and the onset-delay binaural stimuli. In addition, the centers-of-mass for the grand-averaged fMRI activations were practically identical to the corresponding mean locations of the single-subjects' activations.

MEG data

Figures 5 and 6 show the ERF responses over the right hemisphere for a single subject under the different stimulus conditions. The dipolar nature of the components, especially of the M50 and the M100, can be seen, in that these components invert in polarity at anterior sites (e.g., sites 32, 33) relative to the same component at posterior sites (sites 2, 19). This dipolar distribution can be seen even more clearly in the topographic map shown for the M100 for this same subject (Fig. 7). Such a magnetic field distribution is typical for an M100 component and is consistent with a focal dipolar source located in the auditory cortex on the superior temporal plane, oriented perpendicular to the cortical surface.

The amplitudes of the ERF response shown in Figures 5 and 6 can be seen to follow the fMRI patterns, in that the responses appeared to be contralaterally larger for monaural stimuli, with no difference apparent for the laterally perceived binaural stimuli. The grand-averaged responses at the extrema sites (Fig. 8) also show the contralateral predominance of the monaural responses, with little or no difference for the binaurals.

The analysis of the ERF field values confirmed the qualitative convergence with the fMRI results, indicating significant contralaterality of monaural stimulus processing and no contralaterality for the laterally perceived binaurals (Fig. 9). However, the degree of the monaural contralaterality of the MEG recordings was significantly less than the fMRI. In addition, it also

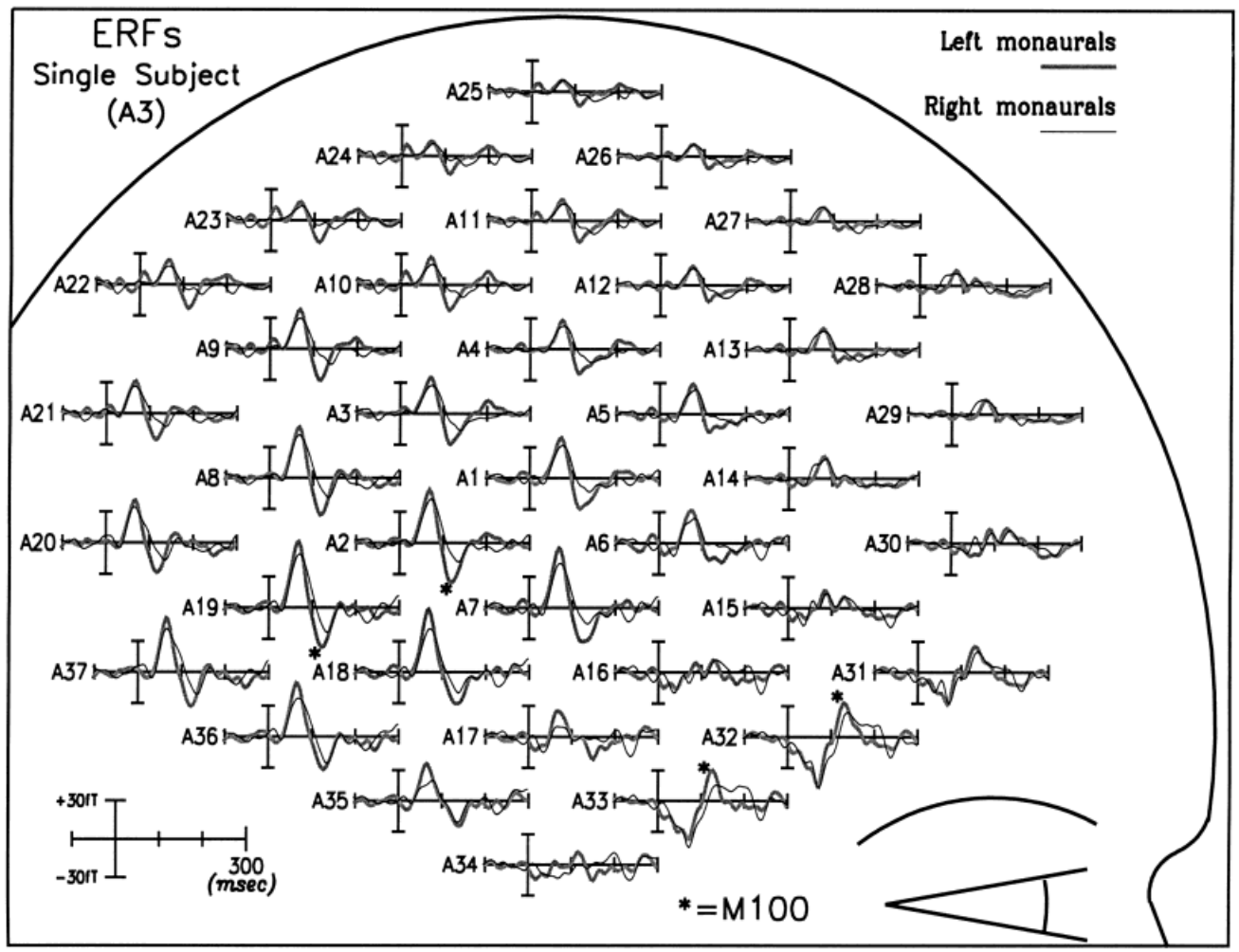

Figure 5.

ERF responses to monaural left and monaural right stimuli over the right hemisphere for a single subject (Subject A3). Note the inversion of the M100 component (asterisks) at the anterior sites (e.g., A32, A33) relative to the posterior sites (e.g., A2, A19), a dipolar distribution that is consistent with a source in the auditory cortex on the superior temporal plane. The contralateral stimulus (left, in this case) can be seen to give clearly larger responses than the ipsilateral (right) one, for both the M100 component peaking at ~120 msec poststimulus and the earlier M50 component peaking at around 60 msec.

varied somewhat depending on the latency range analyzed, with the mean RMS field-value contralaterality indices measuring .57, .55, and .53 for the M50, M100, M200 latency windows, respectively, and .55 for the entire 20–250 ms epoch (Fig. 9), all of which were statistically different from the ipsilateral indices as tested by Wilcoxon matched-pairs signed-ranks test ($P < .0005$ for the M50, M100, and entire epoch window, $P = .03$ for the M200 window). Statistical analyses comparing the RMS contralaterality indices for the entire epoch window to the fMRI contralaterality indices confirmed that the MEG contralaterality was significantly less, at least as assessed by these measures (*t*-test: $P < .001$; Wilcoxon matched-pairs signed-rank tests: $P < .005$). To test whether the degree of contralaterality differed between the different latency windows, matched-pair *t*-tests (with Bonferroni correction for multiple comparisons) of the contralaterality between pairs of the latency windows were also performed. Contrasts between the first two windows (M50 and M100) and between windows 2 and 3 (M100 and M200) did not reach significance ($P = .18$ for both), but the contrast between windows 1 and 3 did so ($P < .002$).

The contralaterality analysis of the dipole strengths of the estimated ECDs fit well with the RMS values,

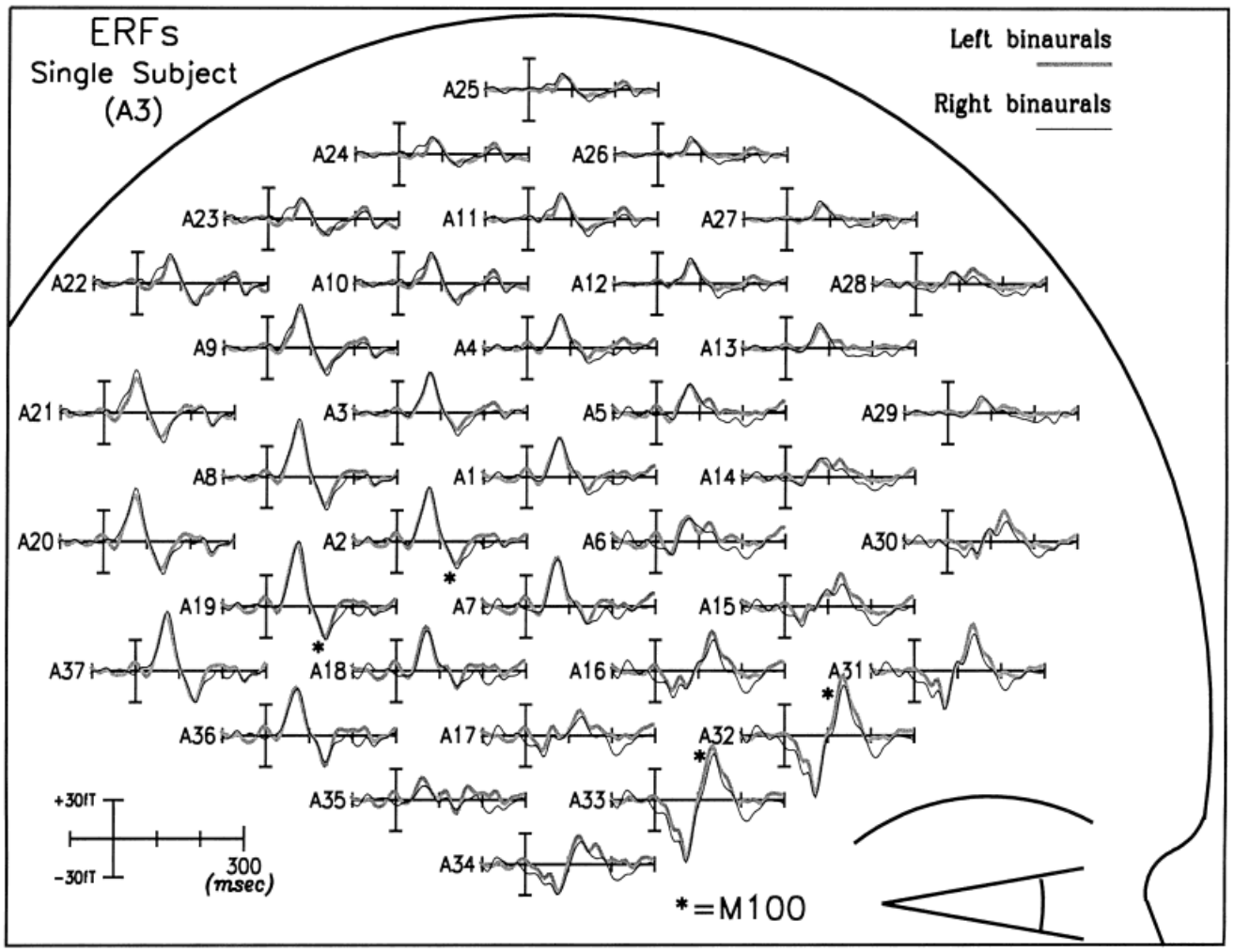

Figure 6.

ERF responses to binaural left and binaural right stimuli over the right hemisphere for the same single subject as in Figure 5 (Subject A3). Note that there was very little difference between the responses to these stimuli, despite their lateralized perception to opposite sides of space.

although the results appeared to be noisier. Due to the neuronal refractoriness resulting from the fast stimulus rate used (3/sec in a single repeated stimulus channel), the evoked responses for a number of the subjects were fairly small. This resulted in the dipole fitting for these subjects being somewhat noisy, which in turn may have caused the contralaterality analysis of the dipole moment amplitudes to be noisier as well. Thus, the contralaterality effect for the dipole moments reached significance (Wilcoxon matched-pairs signed-ranks test) for the M50 analysis (P = .025), but only approached significance for the M100 (P = .07). Nevertheless, these ECD analyses for the M50 and M100 components yielded very similar means across subjects of the contralaterality indices (.58 for the M50 and .55 for the M100) as those derived from the RMS calculations. Likewise, the means of M50 and M100 dipole moment strength contralaterality indices for the binaural stimuli were also similar to the corresponding RMS indices, averaging very near .50, with neither significantly larger contralaterally. The dipole analyses of the M200 did not yield good fits for many of the subjects in this experiment, again probably because of the relatively small magnitude of the M200 waves at the fast stimulus rate used, and therefore dipole moments for this later component were not analyzed.

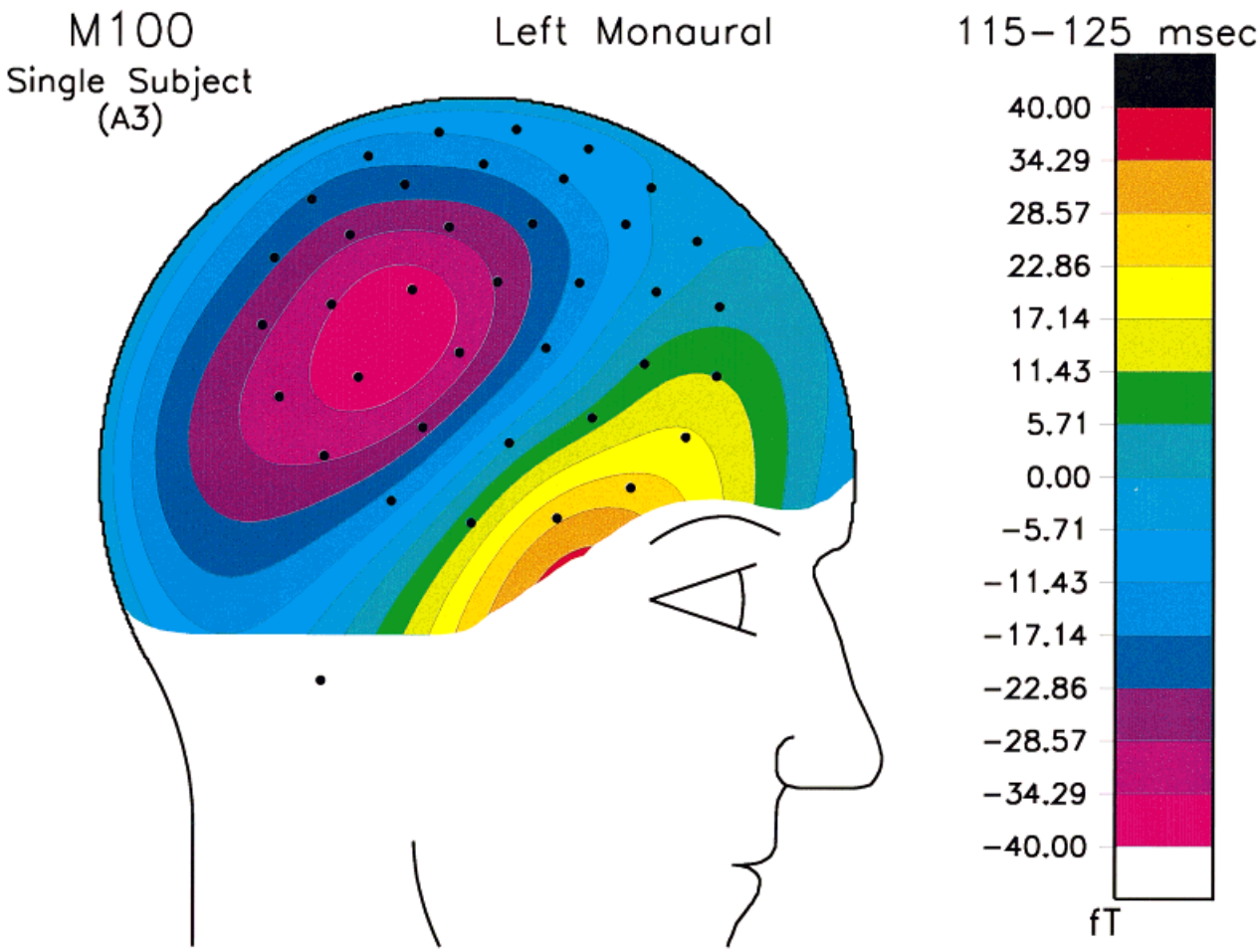

Figure 7.
Topographic map of the magnetic field distribution for the M100 elicited by left monaural stimuli, shown for the same subject whose waveforms are shown in Figures 5 and 6. The dipolar distribution of this response can be clearly seen, with a field maximum anteriorly and a field minimum posteriorly. This dipolar distribution over the temporal lobe is a hallmark of the M100, which is typically well-modeled as arising from a single focal dipolar source in auditory cortex.

Figure 9 suggests that there was a latency difference between the contralateral and ipsilateral monaural responses for the M50 and the M100, besides whatever amplitude differences there were. This was tested statistically by measuring the peak latency for these components in their respective windows, at the sites with the largest responses, which were typically from the posterior extremum. ANOVA indicated that the response to a stimulus in the ipsilateral ear was significantly delayed in latency by 11.0 msec for the M50 ($P < .007$) and 8.5 msec for the M100 ($P < .04$).

Figure 10 shows an example of the estimated centroids of the MEG and fMRI activations for a single subject. Shown in a right sagittal view through auditory cortex is the location of the ECD for the M100 for left monaural stimuli, along with the centroid of the corresponding fMRI activation for those same stimuli for the same subject.

Additional analyses to examine the difference between the fMRI and MEG quantifications of the monaural contralaterality

Because MEG selectively detects activity within sulci and is relatively blind to activity on the

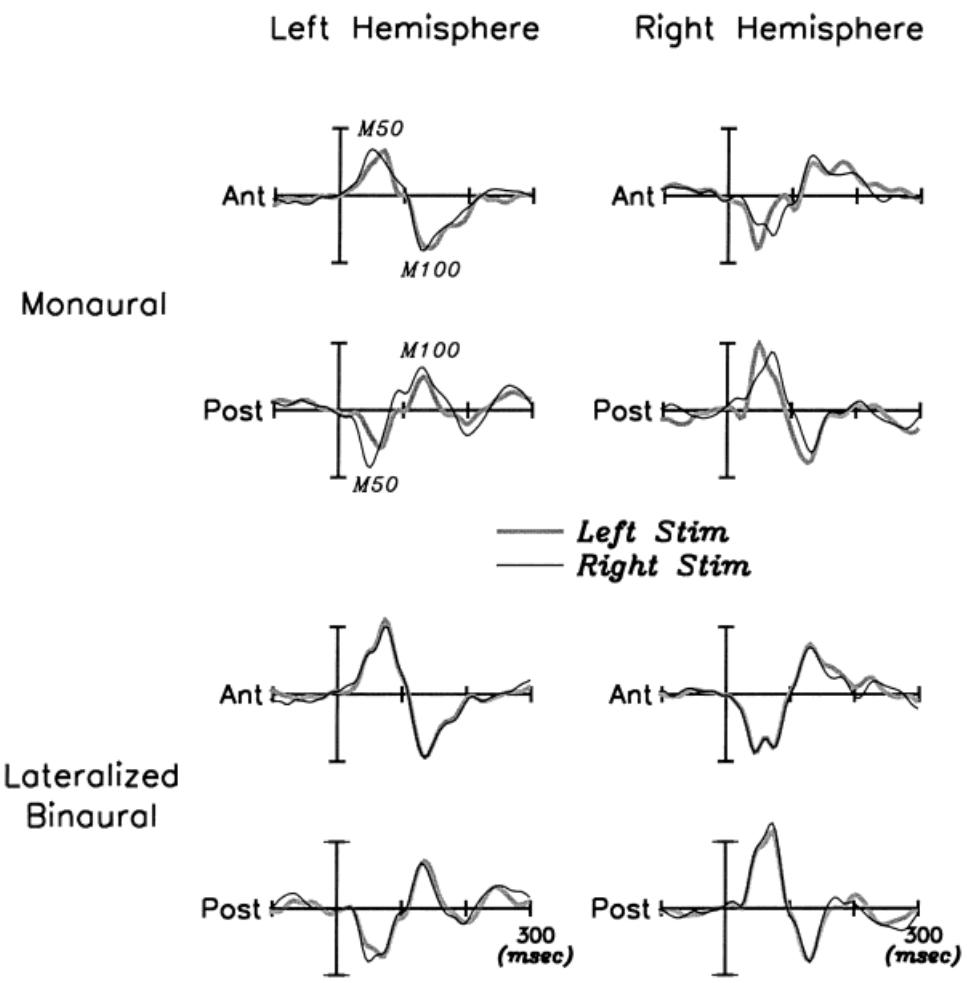

Figure 8.

The grand-averaged ERF responses at the extrema sites. These were derived by extracting the ERF responses at the field maximum site and the field minimum site for each stimulus type, for each hemisphere, for each subject, and then averaging these across subjects. Note the larger amplitude (and earlier latency) for the contralateral monaural responses, with little or no effect of contralaterality for the laterally perceived binaurals.

gyral convexities, it is conceivable that this could have caused the quantitative difference between the fMRI and MEG contralaterality values for the monaural stimuli (.67 vs. .55). To test for this, the fMRI activations were also analyzed with the lateral surface of the superior temporal gyrus excluded in order to match the most likely potential MEG activation sources as best as possible. (This entailed excluding the lateral 3 pixels (7.5 mm) from the ROIs.) However, this analysis resulted in a very slight *increase* (from .67 to .70) in the mean contralaterality indices for the monaurals (the change of which was significant:$P < .01$) and no significant change for the binaurals. Since this small increase for the fMRI monaural indices only served, if anything, to slightly increase the difference between the fMRI and the MEG indices, the difference in gyral sensitivity for fMRI and MEG could not have been the source of the modality quantification difference here.

Another point to consider about the fMRI/MEG contralaterality measures concerns the thresholding used for the fMRI. Using a threshold of $P < .01$ vs. $P < .05$ yielded the contralaterality measures of .67 and .61, respectively; the latter of these is certainly closer to the MEG value. One

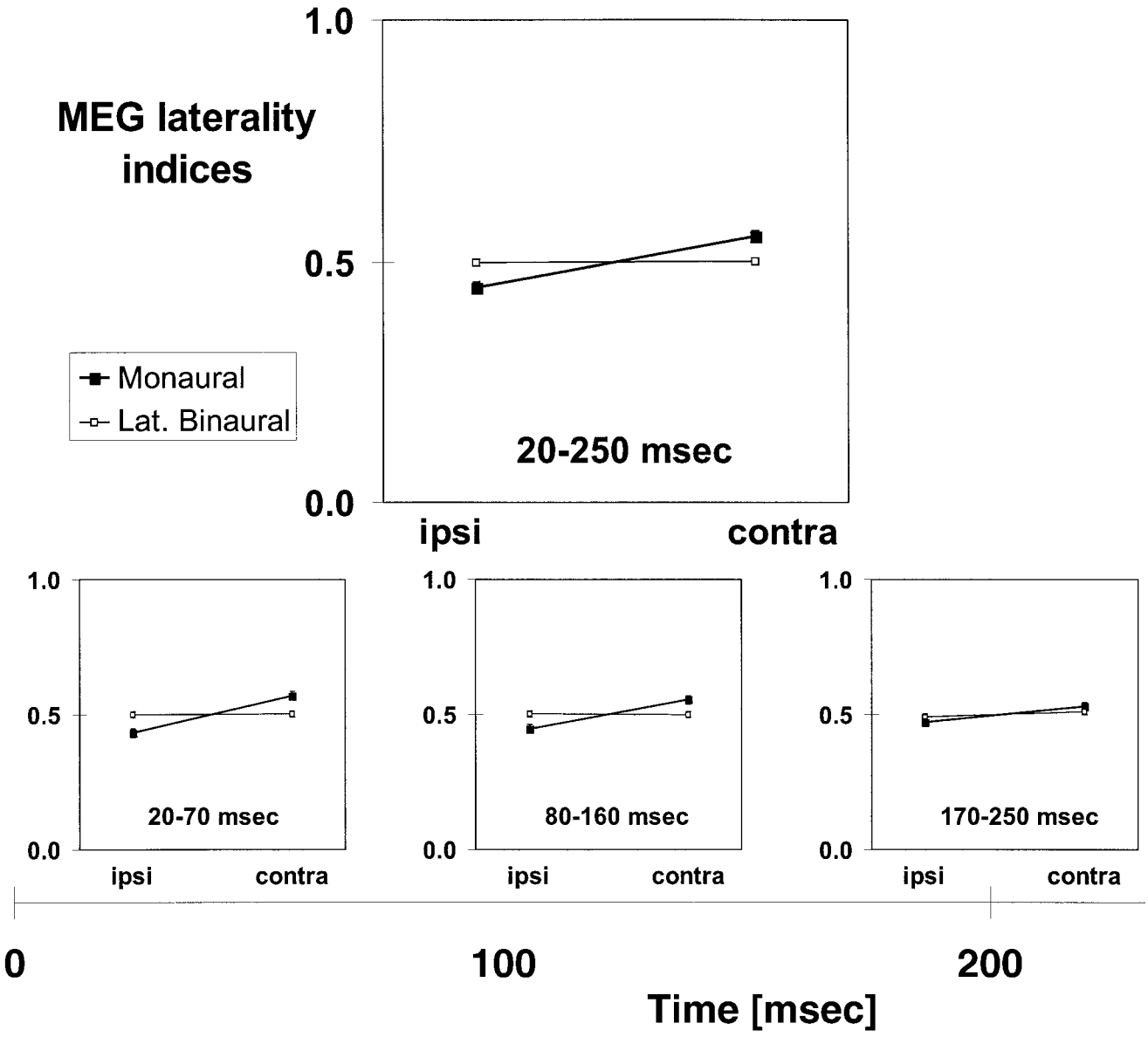

Figure 9.

Plots of the mean MEG contralaterality indices (with SEM error bars) for the different stimulus types, derived from the RMS of the responses across the channels and across various latency windows. These are shown for the overall epoch (20–250 msec), as well as for the latency windows centered on the M50 (20–70 msec), M100 (80–160 msec), and M200 (170–250 msec) components. Note the contralaterality for the monaural stimuli, which decreases across time, and the lack of contralaterality for the laterally perceived binaural stimuli.

possible cause for this thresholding-level effect in the fMRI is that some pixels could have been activated by both contralateral and ipsilateral monaural stimuli, but with the contralateral effect being stronger. Therefore, there could have been pixels in which the contralateral stimulus effect reached significance but the ipsilateral one did not. In the higher-threshold (.01) analysis, this could have resulted in these pixels being included in the contralateral activation measure but excluded from the ipsilateral one,

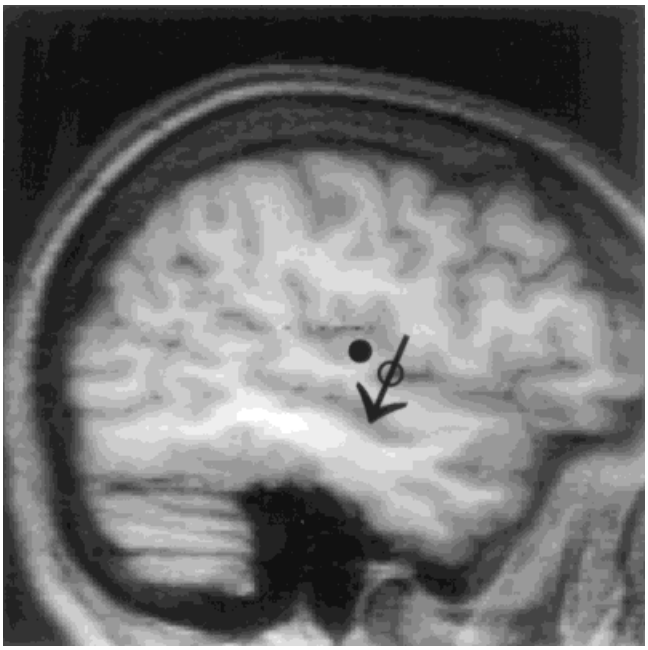

Figure 10.
Example of fMRI and ERF activity centroids for left monaural tones for a single subject, shown on a sagittal MR image through right auditory cortex. Filled circle shows location of intensity-weighted centroid of fMRI activation, and arrow with open circle shows the calculated ECD for the M100 component at 120 msec. The orientation of the ECD arrow indicates the calculated orientation of the dipole, and the open circle at its center identifies the calculated location. The sagittal slice is 47 mm right of the midline.

thereby overemphasizing the contralaterality for that analysis. On the other hand, in the lower-threshold (.05) analysis some additional pixels will show significant activation increases simply by random chance alone, and these would tend to artifactually dilute, and thus decrease, the true contralaterality index in that analysis.

To test for these possibilities, an additional analysis was done on the monaural responses. Theoretical considerations imply that at $P < .05$ and at $P < .01$ there will be, on average, a certain number of pixels significantly ''activated'' by chance alone: namely, 5% and 1% of the total number of pixels in the ROIs. By subtracting these ''false-positives'' from the total number of activated pixels for each subject, the noise-dilution effect of the thresholding could be approximated and eliminated. (Note that in this calculation, we do not know *which* of the pixels were the false-positive ones, just approximately how many there were likely to have been.) This adjustment calculation was applied to both the .05 and the .01 monaural analyses, and the resultant contralaterality indices were found to now be very similar, with both being slightly higher than the unadjusted .01-analysis value of .67. If the adjusted value for the .05 analysis had been close to the original value for that analysis (i.e., .61), then this would have indicated that the random-chance false-positive pixels in that analysis did not contribute much to this analysis giving a lower contralaterality value. In contrast, since the adjusted .05-analysis and .01-analysis values were both close to the original .01-analysis value, this suggests that the false-positive pixels in the .05 analysis were substantially artifactually diluting the contralaterality estimate in that analysis, and that the true value is more likely to be close to the .01-analysis value of .67. Correspondingly, this also implies that the higher thresholding in the .01 analysis did not result in a significant number of pixels reaching significance with contralateral stimulation but not ipsilateral. Thus, these results would also appear to indicate that the thresholding in the fMRI analysis is not the source of the contralaterality quantification differences between the fMRI and the MEG.

DISCUSSION

The present results provide a quantification of the degree of contralaterality in the auditory pathways in humans, as well as information concerning the locus and mechanism of the lateralized perception of onset-delay binaural stimuli, and thus of spatially lateralized real-world sounds. The measures of contralaterality were obtained by both hemodynamic and electromagnetic means, the results of which closely paralleled one another qualitatively, but differed quantitatively.

In terms of the auditory pathways, the fMRI results indicate a relatively high degree of contralaterality — approximately 2:1 — in monaural activation of auditory cortex, at least as gauged by the hemodynamic measure of BOLD fMRI. The contralaterality percentage of 67% (from the $P = .01$ fMRI analysis) is somewhat larger than that given by previous MEG and intracranial recording studies, as well as that given by the current MEG results, but appeared to be both consistent and robust. In sharp contrast, there was no significant contralaterality in the fMRI responses to the

onset-delay binaural stimuli, despite their lateralized perception.

The MEG recordings from these same subjects during the same stimuli and task also indicated a clear contralaterality of the monaural stimulus processing, with essentially no contralaterality for the laterally perceived binaurals. The exact degree of the MEG monaural contralaterality varied somewhat, depending on which aspect of the data was analyzed: 57% for the RMS field values in the M50 latency range, 55% for the M100, 53% for the M200, and 55% for the entire 20–250 msec epoch. The dipole-moment-strength analysis, although weaker statistically, was quite congruent with the RMS analysis, giving contralaterality values of 58% for the M50 and 55% for the M100. The values for the M100 found here match fairly closely previous MEG studies assessing auditory cortex contralaterality. Pantev et al. [1986] reported M100 peak amplitude differences of ~25%, which would correspond to a contralaterality index (as defined here) of ~56% (1.25 / (1.25+1.00)). Makela et al. [1993], using a 122-channel, full-head MEG gradiometer, reported similar M100 contralateral/ipsilateral percentage differences (22–30%), while also reporting similar differences in dipole moment strengths of estimated ECDs (25–30%).

In addition to the contralaterality measures separately supplied here by the fMRI and the MEG, the MEG also suggested that there may be some temporal structure to the contralaterality effect. More specifically, the degree of contralaterality decreased across the epoch, with the pairwise analysis indicating a significant decrease in contralaterality from the M50 window to the M200 window. We would infer that this results from the earliest activity entering auditory cortex from the brainstem being the most contralateral, and then this contralaterality being diluted across time by interhemispheric transfer via the corpus callosum.

There was also a small, but significant latency difference between the contralateral and ipsilateral peaks of the M50 (11 msec) and the M100 (8.5 msec). These values are in the same range as those previously reported in the literature [e.g., Makela et al., 1993]. We presume that these differences in timing of the major activations of the auditory cortices (at least as reflected by the activity that we measure with MEG) result from the bulk of the information inflow arriving into the contralateral auditory cortex earlier than into the ipsilateral auditory cortex, either because of delays or inhibitions in the ascending pathways to the auditory cortex, or delays due to interhemispheric information transfer across the corpus callosum.

Although the fMRI and the MEG results agreed qualitatively on the processing contralaterality of both the monaural and laterally perceived binaural stimuli, the two measures differed substantially in their quantification of the degree of monaural contralaterality. The lesser contralaterality for the MEG did not appear to result from its sulcal selectivity, because a separate analysis of the fMRI after explicitly excluding the main contributing gyral tissue (i.e., the lateral surface of the superior temporal gyrus) did not yield significantly different values. Our additional analysis of the effects of thresholding in the fMRI would also appear to rule out thresholding as causing an overestimate of contralaterality.

On the other hand, because fMRI integrates activity over an extended time period, the quantification difference could have resulted from sustained activations being detected in the fMRI but not in an evoked MEG transient, such as sustained effects of attention to one ear or one side of auditory space enhancing the *background* contralateral activity. However, if such an effect occurred, it did *not* show up in the activations for the laterally perceived binaurals, for which the same attentional tasks were performed on a laterally perceived auditory stimulus channel.

Another possible source of the monaural contralaterality differences could be that during the fMRI scanning there was substantial acoustic noise from the scanning process, whereas there was no such background noise during the MEG recordings. Although a conventional gradient-echo sequence (FLASH) was used here — which causes considerably less acoustic noise than would typically have been the case with echo-planar imaging — and acoustic insulation was used to muffle the noise as much as possible, there was still nonnegligible background sound during the fMRI that was not occurring during the MEG.

Thus, although several technical sources of the fMRI–MEG differences could be ruled out, there are several other possible causes of these differences that may require further investigation. Another possibility to consider, however, is that the fundamental differences between what these methodologies detect means that their typical measures (even widely used ones) that assess contralaterality or other activity strength differences will just tend to have some sort of intrinsic

scaling differences that may need to be sorted out. Lastly, however, it is important to consider that such differences between the measures, rather than just reflecting some scaling differences of the metric, reflect some fundamental physiological nonlinearities in how electrical/magnetic activity in the neuronal assemblies is mapped to, or ramifies into, hemodynamic changes.

Regardless of the fMRI/MEG differences in the quantification of the degree of monaural contralaterality, the two techniques converged quite closely in indicating a clear contralaterality for monaural activations and thus of the basic auditory pathways, but little or none for the laterally perceived binaurals. Considering the unequivocal and substantial monaural contralaterality, this lack of contralaterality of the laterally perceived binaurals was rather striking. One might have predicted clear contralaterality for the laterally perceived binaurals as well, although perhaps somewhat less than that for the monaurals because the perceptual lateralization is somewhat less. Such contralaterality could have resulted, for example, from some sort of onset-delay-induced modulation of the net output from the brainstem, which analyzes interaural time delays as early as the superior olive. Moreover, the fact that *damage* to an auditory cortex *diminishes* the ability to localize (and attend to) sounds within contralateral space [Jenkins and Masterton, 1982; reviewed in Pickles, 1981; King and Carlisle, 1995] might have meant that the process of an intact auditory cortex *perceiving* and attending to sounds in contralateral space would have led to *more* population activity than in the ipsilateral cortex. This was not the case in the present experiment, however, and thus the strongly lateralized perception of these binaural sounds apparently does not arise from any significant contralateral predominance of activation in auditory cortex, either in the overall integrated activity seen in the fMRI, nor in any of the three main phases of the evoked MEG transient responses arising from auditory cortex. Although it is conceivable that this study simply lacked sufficient statistical power to detect a contralaterality of processing, there certainly was more than sufficient power to clearly demonstrate substantial contralaterality of monaural processing, using both of these very different techniques. Thus, the question still remains as to the mechanism and/or locus of the lateralized perception of the onset-delay binaurals.

One possible way to interpret the contralaterality patterns in the present experiment may derive from considering some known binaural neuronal mechanisms in auditory cortex [for a review, see Clarey et al., 1992]. The two principles of sound localization, i.e., by interaural level difference (ILD) or by interaural time difference (ITD), have been found to be represented in primary auditory cortex of various animals mainly by two types of units, those sensitive to ILD (~65% of binaural units) and those sensitive to ITD (~35%). Most ILD-sensitive neurons are of the EI binaural type (excited by the contralateral ear and inhibited by the ipsilateral ear), whereas most ITD-sensitive neurons are of the EE binaural type (excited by both ears but somewhat more by the contralateral ear). Only 10–20% of cortical neurons show no evidence of binaural interaction and are mostly of the contralateral excitation type.

In the light of these neuronal sensitivities, the monaural stimuli — which by definition involved maximal ILDs — may have produced asymmetric hemispheric activation because they stimulated the large population of contralaterally excitatory EI neurons (as well as the small population of *monaural* contralaterally excitatory neurons). Activity of the smaller population of binaural excitatory EE neurons, on the other hand, was presumably balanced between hemispheres. The sum of these effects might explain the substantial lateralization for the monaural processing.

In contrast, the laterally perceived onset-delay binaural stimuli would have necessarily mainly involved ITD effects and, therefore, presumably mainly the EE neuronal system. In this case, since both ears were being stimulated, the activity of the large population of EI neurons (as well as the monaural neurons) might have been symmetric. EE neurons should have shown stronger activity contralateral to the leading ear, but perhaps only those sensitive to delays near the chosen one (2 msec). Such a scenario could explain the negligible hemispheric asymmetry, despite the strongly lateralized perception.

On the other hand, in several recent studies a Finnish MEG group *did* report significant contralaterality for onset-delay binaurals for the M100 wave [McCevoy et al., 1993, 1994], with the degree of contralaterality (in terms of the indices used here) being ~57% for the M100 (and ~54% for the M50). It is not clear why our binaural results do not match these previous ones, but there were several key differences in the parameters: these previous experiments 1) used click-train stimuli, with each click of only ~1 msec

duration, whereas we used 22-msec FM sweeps, 2) used onset delays that were more physiologically (i.e., real-world) plausible (~.7 msec), rather than the 2-msec ones we used, and 3) had the subjects read a book rather than attend to the stimuli. We have now constructed the stimuli used by the Finns and compared them to ours in a small group of subjects, and the subjective perceptual laterality appeared to be quite similar. However, perhaps the very sharp onset and duration of the click stimuli produce better synchronization of some aspect of the response that results in a contralaterality in the recordings that maps with the lateralized percept. If so, however, this would still not explain the lateralized percept that our FM-sweep stimuli also evoke in a listener. Future research will be required to elucidate the source(s) of these differences and dissociations.

In conclusion, the monaural fMRI and MEG results demonstrated clear contralaterality of auditory cortical processing in humans and provide measures of the degree of this contralaterality. The fMRI measure indicated considerably higher contralaterality (67%) than did the MEG (55%), for reasons as yet to be resolved. In contrast, both the fMRI and MEG indicated no contralaterality of processing for the onset-delay binaural stimuli, despite their strongly lateralized percept. However, if this lateralized perception does not derive from contralateral predominance of auditory cortex activation, it presumably must derive from some mechanism.

We consider that there are several main possibilities for alternative mechanisms, which we tend to assume still occurs in cortex. One possibility is that only a very small focal portion of auditory cortex actually is contralaterally more active for these onset-delay binaural stimuli. It is possible that this contralaterally more active portion might help to subserve the lateralized perception, but its area or effect may be so small, at least in the present study, that it was just too highly diluted in an ROI analysis that covered the entire auditory cortex. Another possible explanation for the lateralized perception is that it derives from the contralaterality of processing in higher-level areas not recorded in this study. And, lastly, an important possibility to consider is that the lateralized perception is constructed or represented in some other, more subtle, way from the combined processing of the auditory cortices on both sides of the brain.

ACKNOWLEDGMENTS

We thank Drs. H. Mayberg, J.H. Gao, M. Liotti, and G.R. Mangun for helpful comments on earlier versions of the manuscript.

REFERENCES

Binder JR, Rao SM, Hammeke TA, Frost JA, Bandetinni PA, Hyde JS (1994): Effects of stimulus rate on signal response during functional magnetic resonance imaging of auditory cortex. Cogn Brain Res 2:31–38.

Blauert J (1997): Spatial Hearing: The Psychophysics of Human Sound Localization. Cambridge, MA: MIT Press.

Brodal A (1981): Neurological Anatomy. New York: Oxford University Press, pp 602–639.

Celesia GG (1976): Organization of auditory cortical areas in man. Brain 99:403–414.

Clarey JC, Barone P, Imig TJ (1992): Physiology of thalamus and cortex. In: Popper AN, Fay RR (eds): The Mammalian Auditory Pathway: Neurophysiology, New York: Springer, pp 232–334.

Hamalainen M, Hari R, Ilmoniemi RJ, Knuutila J, Lounasmaa OV (1993): Magnetoencephalography: Theory, instrumentation, and applications to noninvasive studies of the working human brain. Rev Mod Phys 65:413–497.

Irvine DRF (1992): Physiology of the auditory brainstem. In: Popper AN, Fay RR (eds): The Mammalian Auditory Pathway: Neurophysiology. New York: Springer, pp 153–231.

Jenkins WM, Masterton RB (1982): Sound localization: Effects of unilateral lesions in central auditory system. J Neurophysiol 47:987–1016.

King AJ, Carlisle S (1995): Neural coding for auditory space. In: Gazzaniga M (ed): The Cognitive Neurosciences. Cambridge, MA: MIT Press, pp 665–681.

Lauter JL, Herschovitch P, Formby P, Raichle ME (1985): Tonotopic organization in the human auditory cortex revealed by positron emission tomography. Hear Res 20:199–205.

Makela JP, Ahonen A, Hamalainen M, Hari R, Ilmoniemi R, Kajola M, Knuutila J, Lounasmaa OV, McEvoy L, Salmelin R, Salonen O, Sams M, Simola J, Tesche C, Vasam JP (1993): Functional differences between auditory cortices of the two hemispheres revealed by whole-head neuromagnetic recordings. Hum Brain Mapp 1:48–56.

Marquardt DW (1963): An algorithm for least-squares estimation of nonlinear parameters. J Soc Ind Appl Math 11:431–441.

McCevoy L, Hari R, Imada T, Sams M (1993): Human auditory cortical mechanisms of sound lateralization. II. Interaural time differences at sound onset. Hear Res 67:98–109.

McCevoy L, Makela JP, Hamalainen M, Hari R (1994): Effect of interaural time differences on middle-latency and late auditory evoked magnetic fields. Hear Res 78:249–257.

Moore B (ed) (1994): Hearing (Handbook of Perception & Cognition). New York: Academic Press.

Naatanen R, Picton T (1987): The N1 wave of the human electric and magnetic response to sound: A review and an analysis of the component structure. Psychophysiology 24:375–425.

Pantev C, Lutkenhoner B, Hoke M, Lehnertz K (1986): Comparison between simultaneously recorded auditory-evoked magnetic

fields and potentials elicited by ipsilateral, contralateral, and binaural tone burst stimulation. Audiology 25:54–61.

Pickles JO (1981): An Introduction to the Physiology of Hearing. New York: Academic Press, pp 195–227.

Robinson SE (1989): Environmental noise cancellation for biomagnetic measurements. In: Williamson SJ, Hoke M, Stroink G, Kotani M (eds): Advances in Biomagnetism. New York: Plenum Press, pp 721–724.

Talairach J, Tournoux P (1988): Co-Planar Stereotaxic Atlas of the Human Brain. New York: Thieme.

Winer JA (1992): The functional architecture of the medial geniculate body and the primary auditory cortex. In: Webster DB, Popper AN, Fay RR (eds): The Mammalian Auditory Pathways: Neuroanatomy. New York: Springer, pp 222–409.

Woldorff MG (1993): Distortion of ERP averages due to overlap from temporally adjacent ERPs: Analysis and correction. Psychophysiology 30:98–119.

Zatorre RJ, Evans AC, Meyer E (1994): Neural mechanisms underlying melodic perception and memory for pitch. J Neurosci 14:1908–1919.